ZnO-nanoparticle-coated carbon nanotubes demonstrating enhanced electron field-emission properties

Joshua M. Green, Lifeng Dong, Timothy Gutu, and Jun Jiao[a)]
Department of Physics, Portland State University, Portland, Oregon 97207-0751

John F. Conley, Jr. and Yoshi Ono
Integrated Circuit Process Technology Group, Sharp Labs of America, Camas, Washington 98607

(Received 4 November 2005; accepted 8 March 2006; published online 12 May 2006)

Multiwalled carbon nanotubes (CNTs) were coated, using atomic layer deposition, with a thin layer of ZnO and subsequently annealed. Studies of the morphologies of the ZnO-coated CNTs revealed no significant change in the internal structures (multiwalled graphite sheets) and the diameters of the CNTs, but the ZnO appeared to form bead-shaped single crystalline particles attaching to the surface of the nanotubes. The electron field-emission properties of the ZnO-coated CNTs were dramatically improved over both uncoated CNTs and ZnO nanowires. It is reasoned that numerous ZnO "nanobeads" on the surface of the nanotubes serve as additional emission sites, in addition to the tips of CNTs, and result in the enhancement of electron field emission. © *2006 American Institute of Physics*. [DOI: 10.1063/1.2194112]

I. INTRODUCTION

Since their discovery in 1991,[1] carbon nanotubes (CNTs) have been investigated as electron field-emission sources for use in devices ranging from flat-panel displays to electron microscopes.[2–6] Various methods, such as arc discharge, laser ablation, and chemical vapor deposition (CVD), have been used to synthesize CNTs. Among these methods, CVD is an effective way to synthesize patterned thin films of multiwalled CNTs. Also, many studies have investigated the electron field-emission characteristics of CNTs such as turn-on field, threshold field, and field enhancement factor.[7–9] In addition, ZnO nanowires have been shown to have not only superior optical properties[10] but also promising field-emission characteristics since the nanowires have structural morphologies similar to those of CNTs, such as a high aspect ratio and small radius.[11]

In this study, we combined these two unique materials together in the form of ZnO-coated CNTs and investigated their electronic properties. This approach not only resulted in exotic morphologies of ZnO-coated CNTs but also significantly enhanced their electron field-emission properties.

II. EXPERIMENT

CNTs were grown using Fe as a catalyst, as previously reported.[12] Silicon substrates coated with Fe catalyst were placed in a ceramic boat in a quartz tube, which was placed in a horizontal tube furnace. To synthesize CNTs, three steps were performed: (1) calcination of the catalyst at 450 °C for 2 h at 3×10^{-2} Torr, (2) activation of the catalyst at 500 °C and at 75 Torr of H_2 for 30 min, and (3) carbon nanotube growth at 700 °C at 75 Torr of an admixture of H_2 [385 SCCM (standard cubic centimeter per minute at STP)] and C_2H_2 (25 SCCM) for 30 min. After the growth period, the reaction chamber was evacuated to 3×10^{-2} Torr and allowed to slowly cool. When the reactor reached room temperature, the chamber was vented and the samples were removed. Then the CNTs were coated with ZnO using atomic layer deposition (ALD) with diethylzinc and H_2O as precursors and subsequently annealed. The annealing was performed in N_2 at 900 °C for 60 s.

All the samples were characterized by means of the following techniques: An FEI Sirion field-emission scanning electron microscope (FESEM) operating at 15 kV was used to study the morphology of the samples; an FEI Tecnai F-20 field-emission high-resolution transmission electron microscope (HRTEM), equipped with an energy-dispersive x-ray (EDX) spectrometer, was used to characterize the internal structures of the coated nanotubes and to analyze their elemental compositions.

Field-emission experiments were performed in an ultrahigh vacuum (UHV) chamber, with a base pressure of $<1\times10^{-9}$ Torr, at room temperature. The test system had a point-to-plane geometry between a tungsten anode probe tip with a radius of 25 μm and the planar cathode, a silicon substrate on which the ZnO-coated nanotubes were located. The silicon substrate was attached to a movable stainless steel plate with silver paste, and connected to a picoammeter for the emission *I-V* measurements. The probe was connected to a high-voltage power supply. Since the cathode plate was connected to a micromanipulator, the position of the nanotubes with respect to the anode probe was variable. This enabled the point-to-plane separation to be adjusted from 100 to 300 μm, which was considerably larger than the radius of the probe tip.

III. RESULTS

Figure 1(a) shows a FESEM image of the as-made CNT film, while Fig. 1(b) displays the CNT film after the ALD of ZnO. Note that a thin layer of ZnO is visible on the surface of CNTs. Figure 1(c) reveals the morphology of ZnO-coated

[a)]Electronic mail: jiaoj@pdx.edu

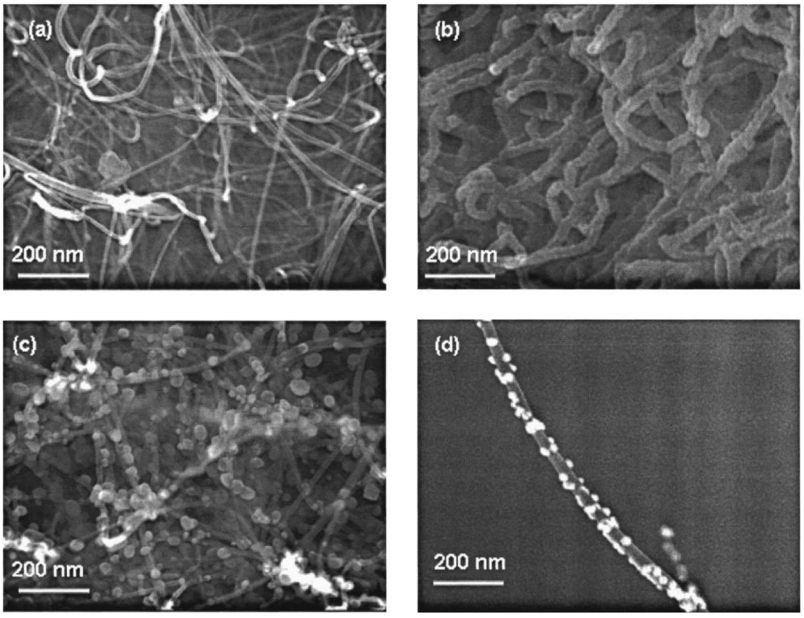

FIG. 1. SEM images of (a) as-synthesized CNTs, (b) some carbon nanotubes coated with a thin layer of ZnO after ALD of ZnO, (c) carbon nanotubes coated with ZnO beads, after the annealing process, and (d) an isolated nanotube bundle coated with numbers of bead-shaped particles after the ALD process and without the annealing process.

CNTs after annealing. Although there appears to be no significant change in the morphology of the CNTs themselves (for instance, the diameter of the tubes remains approximately the same), strikingly, numerous particles appear on the surface of the nanotubes like beads on a necklace. A systematic characterization of the ZnO-coated nanotube samples suggests that the bead-shaped particles can also form on the surface of the CNTs during the ALD process without going through the annealing process, as in Fig. 1(d). However, in most of the samples, the ALD of ZnO results in a thin layer of ZnO on the surface of the nanotubes as indicated in Fig. 1(b). After annealing, this thin layer transforms into bead-shaped particles as shown in Fig. 1(c). Although it is not clear why bead-shaped particles can also be found in unannealed samples, we have discovered that when using diethylzinc and H_2O chemistry for ALD, the initial nucleation of ZnO is extremely sensitive to surface conditions. Additionally, it has been reported that it is difficult to initiate ALD on CNTs because of the closed bonding and that defects sites are likely responsible for nucleation.[13,14] It is thus possible that the inhomogeneity of carbon nanotube film contributes to the formation of different morphologies of ZnO coating on the nanotube surface in different sample areas. This speculation was supported by the observation of as-coated samples where the bead-shaped particles appeared on the surface of some nanotubes, while other nanotubes were coated with a thin film of ZnO. After the annealing process, however, the presence of the bead-shaped particles was more uniform, and the particles were more consistent in size and shape.

To further understand the internal structure of the ZnO-coated CNT, we used the TEM to characterize the samples. The TEM image in Fig. 2(a) shows several of the "beads" that were formed on the surface of the tube after the annealing process. A thin amorphous layer appeared on the surface of the tube as well. Figure 2(b) reveals the graphitic structure of the CNT while also showing that the ZnO particle appears to slightly deform the nanotube. Figure 2(c) is a HRTEM image of a ZnO nanoparticle attached to a nanotube. The lattice fringes of the particle indicate the single crystallinity of the particle. Note that the shape of the particle in Fig. 2(c) is polyhedral rather than spherical. The diameter of the particle is comparable to that of the attached nanotube. Our overall TEM observation suggests that, although some of the beads are approximately spherical, many of them are polyhedral. The size of most particles is in the range of the diameters of the nanotubes, ~10–30 nm.

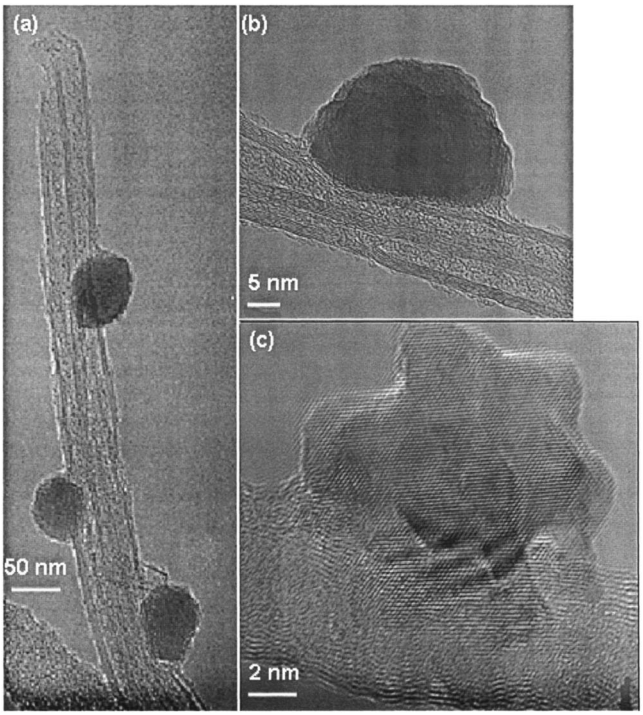

FIG. 2. TEM image of (a) a bundle of CNTs with several ZnO particles attached to it after the annealing process, (b) a large ZnO particle annealed to the sidewall of the nanotube causing the deformation of the tube, and (c) a HRTEM image showing the lattice fringes of the ZnO particle of polyhedral shape.

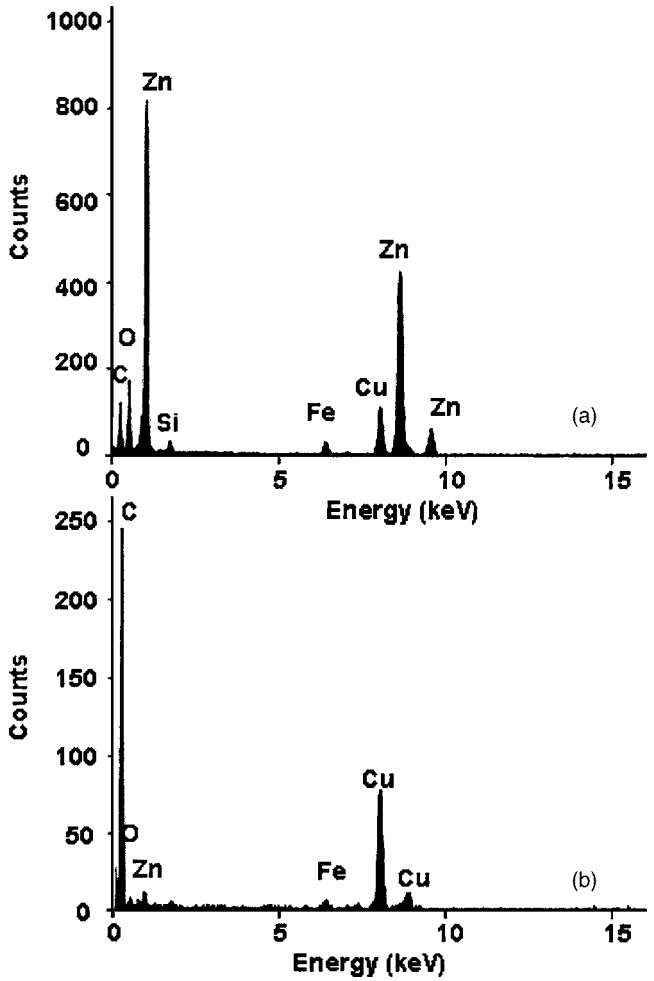

FIG. 3. (a) EDX spectrum obtained by placing the EDX nanoprobe on the ZnO "bead." The carbon signal is from the CNT while the strong signals of Zn and O are from the particle. (b) EDX spectrum acquired by putting the EDX nanoprobe on the CNT only. The strong carbon signal and very weak Zn and O signals suggest that most of the ZnO coating is in the form of particles rather than a thin film. In both spectra, the copper signal is from the TEM grid. The very weak signals of Fe and Si are contributed by the Fe catalysts, which lead the nanotube growth, and the Si substrate where the nanotubes were scraped off for the TEM and EDX analyses.

To further confirm the chemical composition distribution in the ZnO-coated CNT, the EDX nanoprobe equipped in the TEM was placed on one of the beads, where the strong signals of Zn and O were detected as shown in Fig. 3(a). This analysis, along with the HRTEM images showing the lattice fringes of the particles, confirmed that the beads are single crystalline ZnO particles. When the probe was placed away from the beads but on the nanotube, a very weak Zn signal along with very strong carbon signals was detected as indicated in Fig. 3(b). This further confirms that most of the ZnO coating formed ZnO particles attached to the CNTs.

Field-emission measurements suggest that the ZnO coating has a profound effect on the electron field-emission of ZnO-coated CNTs. The results of field emission measurements on ZnO-coated CNTs, uncoated CNTs, and ZnO nanowires are summarized in Table I. Discussion of these results requires the definition of several parameters. The turn-on and threshold fields of an emitter are defined as the macroscopic external field required to extract a current density of

TABLE I. A comparison of field-emission characteristics from various nanostructures.

Sample	Turn-on field ($V/\mu m$)	Threshold field ($V/\mu m$)	Enhancement factor
Uncoated CNTs with Fe catalyst	4.9	6.0	800
ZnO nanowires with Pt catalyst	9.3	14.4	530
ZnO-coated CNTs with Fe catalyst	3.75	5.0	1920

10 $\mu A/cm^2$ and 10 mA/cm^2, respectively. Current density J is defined as $J=I/\alpha$. Here, I is the emission current in amperes and α is the emission area in square centimeters. The emission area was defined as the area of the anode tip;[15] since the same anode was used for every experiment, this definition did not affect the comparison of turn-on and threshold fields.

As shown in Table I, the turn-on and threshold fields for the uncoated nanotubes were found to be 4.9 and 6.0 $V/\mu m$, respectively, and those for the ZnO nanowires were 9.3 and 14.4 $V/\mu m$.[16] By contrast, the turn-on and threshold fields for the ZnO-coated CNTs after the annealing process were 3.75 and 5.0 $V/\mu m$, respectively, much lower than their counterparts. Also, as seen in Fig. 4, the coated nanotubes achieved a much higher current within a small applied voltage range than did the uncoated nanotubes. This measurement was conducted under the condition that the anode to cathode distance was kept the same for all the samples.

The field-enhancement factor γ was estimated from the Fowler-Nordheim (FN) plots, which correspond to the *I-V* characteristics. Based on the triangular-barrier approximation and the FN model, by using the slope S_{FN} of the FN plot, the factor γ can be calculated from the following equation:[12]

$$\gamma = -0.683\frac{d}{S_{FN}}\phi^{3/2}. \quad (1)$$

In this equation, d is the distance between the two electrodes while ϕ is the work function of the emitters. Using Eq. (1) and the slopes obtained from the FN plots in Fig. 5, the field-enhancement factor γ for uncoated nanotubes was calculated to be 800, while that of nanotubes coated with ZnO nanoparticles was 1920. Since emission currents were

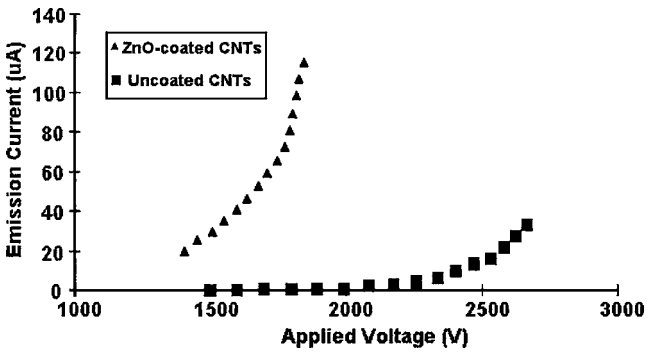

FIG. 4. *I-V* characteristics of uncoated CNTs and ZnO-coated CNTs after the annealing process.

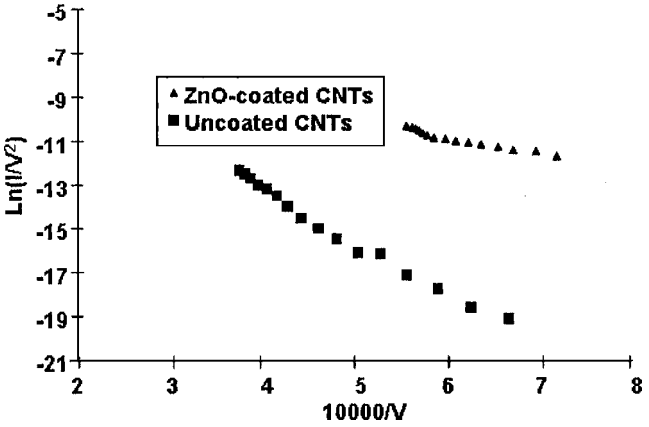

FIG. 5. Fowler-Nordheim characteristics of uncoated CNTs and ZnO-coated CNTs.

measured from many different nanostructures, the values of enhancement factor γ reported here are statistical averages.

IV. DISCUSSION

A plausible explanation for understanding the mechanism resulting in the improvement of the electron field emission by the ZnO-coated nanotubes is given below. The enhancement factor γ has been introduced to reconcile the difference between microscopic and macroscopic fields. As such, it is dependent on the emitter geometry. As suggested by Eq. (1), γ is also related to the work function of an emitter. Since the field-emission characteristics were measured from the films of CNTs, in our calculations the work function of the CNTs was assumed to be 5 eV, as used by other groups.[8] The reported work function of ZnO nanowires is 5.3 eV.[17] Although no direct measurements of work function were performed on the ZnO-coated CNTs, we estimated the work function of this morphology to be 5.15 eV, an average value between 5 and 5.3 eV, to calculate their field-enhancement factor γ. Based on this estimation and Eq. (1), the work function of the ZnO-nanoparticle-coated CNTs does not cause any significant change in the calculated field-enhancement factor γ. Therefore, the significant change in γ must be a result of the change in the geometrical shape of the emitters. Enhancement of field-emission characteristics from a change in geometry has previously been reported in CNTs.[18] This leads us to believe that the bead-shaped ZnO nanoparticles, which have roughly the same diameter as that of CNTs, act as additional emission sites, since their polyhedral shape gives them the advantage of having many sharp tips and edges. Our experiments on some samples where the ZnO coating did not form beads, but instead formed thin coating layers, showed no significant improvement in electron field emission over that of uncoated CNTs. This further confirmed the importance of bead-shaped ZnO nanoparticles for the improvement of the field emission.

Additionally, the morphologies of the CNTs coated with ZnO nanoparticles had an exciting effect on electric field-induced photoemission.[19] It was found that at low fields, an emission spectrum consisted of a sharp 382 nm peak along with a broad peak in the visible region, centered at 508 nm. These emission peaks match the photoluminescence spectra of the thin film ZnO and are not observed in uncoated nanotubes.

In conclusion, this study clearly demonstrates that the field-emission characteristics of CNTs are enhanced by attaching ZnO nanoparticles to them. With these morphologies, ZnO-coated CNTs were found to have lower turn-on and threshold fields, and a significantly improved enhancement factor γ when compared to uncoated CNTs and ZnO nanowires. In addition, the photoemission spectrum of ZnO-nanoparticle-coated CNTs demonstrated the combined properties of ZnO nanowires and CNTs.

V. CONCLUSION

We believe that the beads of ZnO formed by ALD and annealing on the surface of the CNTs are the key to understanding the improved electron field-emission properties. The superb field-emission characteristics of CNTs are known to be related to both work function and geometry. Since the work functions of CNTs and ZnO differ by only 0.3 eV, the differences in work function are not sufficient to explain the dramatically improved field-emission characteristics in ZnO-nanoparticle-coated CNTs. However, since the bead-shaped particles of ZnO are very similar in size to the nanotube tips, they act as additional field-emission sites, thus improving the overall current emitted for a given applied electric field. Our study, therefore, demonstrates a simple way to increase the effectiveness of field emitters by changing their geometrical shapes.

[1] S. Iijima, Nature (London) **354**, 56 (1991).
[2] W. A. de Heer, A. Châtelain, and D. Ugarte, Science **270**, 1179 (1995).
[3] A. G. Rinzler *et al.*, Science **269**, 1550 (1995).
[4] W. B. Choi *et al.*, Appl. Phys. Lett. **75**, 3129 (1999).
[5] N. Jonge, Y. Lamy, K. Schoots, and T. H. Oosterkamp, Nature (London) **420**, 393 (2002).
[6] J. Jiao, L. F. Dong, D. W. Tuggle, C. L. Mosher, S. Foxley, and J. Tawdekar, Mater. Res. Soc. Symp. Proc. **706**, 113 (2002).
[7] W. Zhu, C. Bower, O. Zhou, G. Kochanski, and S. Jin, Appl. Phys. Lett. **75**, 873 (1999).
[8] J. M. Bonard, J. P. Salvetat, T. Stöckli, L. Forró, and A. Châtelain, Appl. Phys. A: Mater. Sci. Process. **69**, 245 (1999).
[9] M. Svenningsson, R. E. Morjan, O. A. Nerushev, Y. Sato, J. Bäckström, and E. E. B. Campbell, Appl. Phys. Lett. **81**, 1095 (2002).
[10] M. Huang *et al.*, Science **292**, 1897 (2001).
[11] L. F. Dong, J. Jiao, D. W. Tuggle, J. M. Petty, S. A. Elliff, and M. Coulter, Appl. Phys. Lett. **82**, 1096 (2003).
[12] L. F. Dong, J. Jiao, C. Pan, and D. W. Tuggle, Appl. Phys. A: Mater. Sci. Process. **78**, 9 (2004).
[13] D. B. Farmer and R. G. Gordon, Electrochem. Solid-State Lett. **8**, G89 (2005).
[14] A. Javey, J. Guo, Q. Wang, M. Lundstrom, and H. Dai, Nature (London) **424**, 654 (2003).
[15] V. V. Zhirnov, C. Lizzul-Rinne, G. J. Wojak, R. C. Sanwald, and J. J. Hren, J. Vac. Sci. Technol. B **19**, 87 (2001).
[16] D. McClain, R. Solanki, L. F. Dong, and J. Jiao, J. Vac. Sci. Technol. B **24**, 20 (2006).
[17] C. J. Lee, T. J. Lee, S. C. Lyu, Y. Zhang, H. Ruh and H. J. Lee, Appl. Phys. Lett. **81**, 3648 (2002).
[18] M. Sveningsson, R. E. Morjan, O. A. Nerushev, E. B. Campbell, D. Malsch, and J. A. Schaefer, Appl. Phys. Lett. **85**, 4487 (2004).
[19] J. F. Conley, Jr., J. Green, L. Dong, J. Jiao, and Y. Ono (unpublished).